International Journal of Rock Mechanics and Mining Sciences 103 (2018) 89–95

Contents lists available at ScienceDirect

International Journal of Rock Mechanics and Mining Sciences

journal homepage: www.elsevier.com/locate/ijrmms

Experimental study and micromechanical interpretation of the poroelastic behaviour and permeability of a tight sandstone

Yi Wang[a], Laurent Jeannin[b], Franck Agostini[c], Luc Dormieux[d], Frédéric Skoczylas[a,c,*], Eric Portier[b]

[a] *School of Civil Engineering and Architecture, Hubei University of Technology, Wuhan, China*
[b] *ENGIE EPI, 1 Place Samuel de Champlain, 92930 La Défense Cedex, France*
[c] *Laboratoire de Mécanique de Lille (LML) CNRS FRE 3723, Centrale Lille, CS 20048, F-59651 Villeneuve D'Ascq Cedex, France*
[d] *ENPC, Institut Navier, 6 & 8 avenue Blaise Pascal, 77455 Marne-la-Vallée, France*

ARTICLE INFO

Keywords:
Tight sandstones
Biot coefficient
Permeability
Micromechanical model
Pore entrapment
Cracks closure

ABSTRACT

This study focuses on the poroelastic behaviour and permeability of tight sandstones, which are characterized by a low porosity, a low gas permeability and a strong sensitivity to in-situ stress. Experimentally the Biot coefficient takes a value close to 1 at low confinement and decreases with increasing confining pressure; the permeability shows an important reduction with increasing confining pressure. This behaviour can be attributed to pore entrapment and to the closure of cracks and joints. Micromechanical models, considering low permeable sandstones as made up of an assemblage of grains with interfaces and pores, reproduce well the observed trends of Biot coefficient and permeability.

1. Introduction

Tight sandstones are usually characterized by a low porosity (lower than 10%), a low gas permeability (less than 0.1 mD) and a strong sensitivity to in-situ stress[1–5]; these rocks are cemented granular rocks[6] and constitute the main reservoir rock of some unconventional tight gas fields.[2] The poroelastic behaviour and mainly the Biot coefficient estimates of tight sandstones are of great practical importance to assess the in-situ stress in reservoirs,[7] and thus to better estimate well stability and design well stimulation processes.

In literature, many efforts have been dedicated to investigate experimentally the poroelastic behaviour and especially Biot coefficient, of different rocks.[8–14] Among which, some studies dedicated to low permeable sandstones[11,13] have reported, that Biot coefficient has a value closed to 1 at low confining pressure and decreases with increasing confining pressure; such decrease is presumably due to the entrapment of a part of initially connected porosity caused by the closure of some pore throats.[8] Besides as observed by Hu et al.,[12] Biot coefficient increases with increasing axial strain due to the propagation of cracks, which may reopen trapped pores. In order to predict Biot coefficient values, Tan et al.[15] proposed a two-dimensional discrete element model, which considers simplified microstructural geometries; Lydzba et al.[16] applied an asymptotic homogenization method. However, both models are not relevant to the pore entrapment phenomenon, which could be an important mechanism for the evolution of Biot coefficient for low permeable sandstones.

Moreover the evolution of permeability for low permeable sandstones is strongly related to the rock's poroelastic behaviour as cracks and joints close under loading.[3,5,11,17–22] Although these joints occupy negligible volume in total pore space, they control the main flow path and the fluid flow.

This work aims at building a simplified model of stress-sensitive Biot coefficient and absolute permeability based on the phenomenons of pore entrapment and joint closure, in order to reproduce the observed trends in experiments. In the first part of this paper, experimental results of Biot coefficient, permeability and porosity under loading are presented. The second part is devoted to a poroelastic model for tight sandstone considered as an assemblage of rigid grains, surrounded by interfaces representing joints. Then, in the last part, based on the derived poroelastic model and the previous work of Dormieux et al.,[6] the stress-sensitive absolute permeability is modeled.

2. Experimental results

In this section we are interested mainly in the experimental characterization of Biot coefficient of tight sandstones at different confining pressure.

For linear poroelastic behaviour, the effective stress is defined by:

---

[*] Corresponding author at: School of Civil Engineering and Architecture, Hubei University of Technology, Wuhan, China.
E-mail address: frederic.skoczylas@centralelille.fr (F. Skoczylas).

https://doi.org/10.1016/j.ijrmms.2018.01.007
Received 8 November 2016; Received in revised form 12 December 2017; Accepted 1 January 2018

$$\sigma^e_{ij} = \sigma_{ij} + bp\delta_{ij} \tag{1}$$

where b denotes the Biot coefficient.

The effective stress depends linearly on the linearized strain ε_{ij} according to the framework of linear poroelastic behaviour.

2.1. Biot coefficient measurements

In our experiments, b is derived as the ratio between two modulus: $b = K_b/H$,[23,24] where K_b denotes the skeleton bulk modulus, which is measured with an decrement in confining pressure ΔP_c ($K_b = \Delta P_c/\Delta\varepsilon_v$, where $\Delta\varepsilon_v$ is the measured volumetric strain increment). H characterizes the volumetric deformation caused by an increment in interstitial pressure ΔP_i ($H = \Delta P_i/\Delta\varepsilon_v$).

The solid matrix bulk modulus K_s is estimated by applying an identical variation in confining pressure and interstitial pressure ($K_s = (\Delta P_c = \Delta P_i)/\Delta\varepsilon_v$).

More specifically we have tested three tight sandstones samples referenced as 2335, 3249 and 3379 and we have chosen four levels of confining pressure: 3 MPa, 10 MPa, 20 MPa and 40 MPa. Under the first confining pressure level, which is considered in this study as the stress-free state, ΔP_c and ΔP_i are chosen to be 1 MPa. Under other confining pressure ΔP_c and ΔP_i are chosen to be 2 MPa to increase measurement accuracy. Computed K_b, H and K_s values are then corresponding to mean confining pressure value $(P_c + P_c - \Delta P_c)/2$.

Fig. 1 displays the experimental results of Biot coefficient of the sandstone samples. We observe that Biot coefficient at initial state (corresponding to a confining pressure of 3 MPa) ranges between 0.87 and 0.97, while it decreases with the confining pressure to values of 0.54–0.56 at 40 MPa.

The observed initial values of Biot coefficient (close to 1) suggest that the samples have large amounts of micro-cracks or joints. When joints get closed gradually during the confining process (see 8) the decrease of Biot coefficient may be attributed to the closure of certain pore throats and to the trapping of some pores, that are now disconnected from the main permeable porous network. In this paper, we focus on the entrapment and joint closure phenomenon and show how they can explain the Biot coefficient and permeability evolution.

2.2. Trapped porosity measurements

Further experiments have been designed to identify the accessible porosity evolution during the confining process (see 25 for a detailed description of the experimental protocol). To assess the part of the porosity that is trapped under loading, we assume that,on one hand, the volume change of joints is negligible,[18] therefore the total porosity variation consists of closed porosity and elastic pore volume change of macropores. On the other hand, at initial state (3 MPa), no pore gets trapped.

The volume balance equation of a poroelastic solid which deforms without pore entrapment writes (see 26)

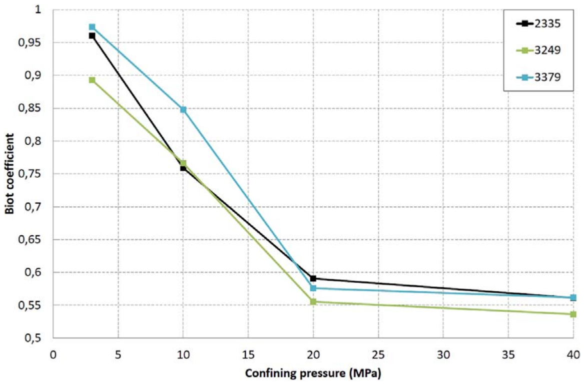

Fig. 1. Biot coefficient under confining pressure.

Table 1
Measurement of bulk volume variation and bulk modulus of solid matrix.

Confining pressure(MPa)	$\Delta\varepsilon_v$(2335)(μdef)	$\Delta\varepsilon_v$(3249)(μdef)	$\Delta\varepsilon_v$(3379)(μdef)
3	0	0	0
10	833	894	1005
20	1622	1528	1658
40	2638	2448	2627

Confining pressure(MPa)	K_s(2335)(GPa)	K_s(3249)(GPa)	K_s(3379)(GPa)
3	31.0	29.1	28.5
10	21.6	20.2	21.7
20	16.8	19.8	19.6
40	26.3	26.9	29.7

$$(1-\phi)\Delta\varepsilon_v = \Delta\phi_e + \frac{\Delta V_{matrix}}{V} = \Delta\phi_e + (1-\phi)\Delta\varepsilon_{matrix} \tag{2}$$

where $\Delta\phi_e$ represents the eulerian porosity variation, $\Delta\varepsilon_v$ represents the bulk relative volume increment, $\Delta\varepsilon_{matrix}$ refers to the solid matrix relative volume increment.

The porosity variation $\Delta\phi_e$ is evaluated from $\Delta\varepsilon_v$ and $\Delta\varepsilon_{matrix}$ for every increment of confining pressure. $\Delta\varepsilon_v$ is directly measured by LVDT sensors, while $\Delta\varepsilon_{matrix}$ for an incremental confining pressure $\Delta\Sigma$ between two confining pressure Σ_f and Σ_i is evaluated by:

$$\Delta\varepsilon_{matrix} = \frac{\Delta\Sigma}{(1-\phi)((K_s(\Sigma_i) + K_s(\Sigma_f))/2)} \tag{3}$$

The values of measured $\Delta\varepsilon_v$ and K_s are reported in Table 1.

The evolution of the trapped porosity $\Delta\phi_p$ related to trapped pores is then estimated by:

$$\Delta\phi_p = \Delta\phi_{measured} - \Delta\phi_e \tag{4}$$

In Fig. 2, the total porosity measured experimentally is represented by solid lines for the three different samples. The estimated decrease of porosity related to poroelastic effects using Eq. (2) is described by dashed lines. Then, the difference between total porosity and the porosity due to poroelastic change is associated with a trapped porosity as a function of confining pressure (see also Table 2).

This interpretation of the porosity evolution in terms of trapped pores related to joint closure is supported also by two other experiments. The first experiment is the measured total porosity in both loading and unloading phases as shown in Fig. 3. We note that the variation of total porosity is largely reversible, which implies that the

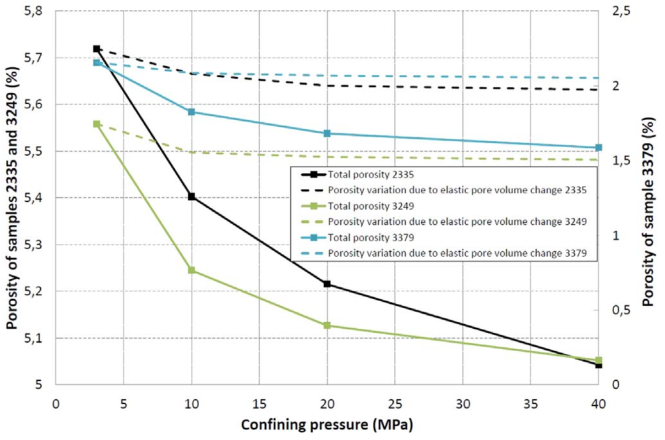

Fig. 2. Total measured porosity (solid line) and estimated porosity poroelastic change (dashed line) under confining pressure - left vertical axis: porosity scale for samples 2335 and 3249 - right vertical axis porosity scale for sample 3379.